Received: 13 February 2017 | Revised: 14 August 2017 | Accepted: 21 August 2017

DOI: 10.1111/ffe.12714

ORIGINAL CONTRIBUTION

WILEY

Effect of 475°C embrittlement on the low cycle fatigue behaviour of lean duplex stainless steels

Renata Strubbia[1] | Mohamed Sennour[2] | Silvina Hereñú[1]

[1]Instituto de Física Rosario-CONICET-UNR, Bv. 27 de febrero 210 bis, 2000 Rosario, Argentina

[2]MINES ParisTech, PSL Research University, MAT-Centre des Matériaux, CNRS UMR 7633, BP 87, 91003 Evry, France

Correspondence
Renata Strubbia, Instituto de Física Rosario-CONICET-UNR, Bv. 27 de febrero 210 bis, 2000 Rosario, Argentina.
Email: strubbia@ifir-conicet.gov.ar

Abstract

Lean duplex stainless steels (LDSSs) with lower nickel and molybdenum are less susceptible to suffer spinodal decomposition than standard duplex stainless steels. It is the purpose of this work to study the effect of thermal embrittlement on the low cycle fatigue behaviour of 2 LDSSs with different Cr_{eq} and Ni_{eq}. The correlation between the fatigue behaviour and the dislocation structure is attempted. Transmission electron microscopy was used to observe the dislocation microstructure. Additionally, STEM-EDS technique in conjunction with Vickers microhardness measurements was used to characterize the amplitude of the spinodal decomposition. The results show that the LDSS with lower Cr_{eq} and Ni_{eq} values exhibits improved fatigue properties in the as received and aged conditions. Furthermore, it is important to emphasize that with an adequate volume fraction of phases in LDSSs, the ageing treatment leads to an increase in strength without causing a great detriment in low cycle fatigue life.

KEYWORDS

dislocations, lean duplex stainless steel, low cycle fatigue, spinodal decomposition

1 | INTRODUCTION

Duplex stainless steels (DSSs) lying midway between austenitic and ferritic stainless steels combine the best properties of both. Its use in different areas of industry (nuclear, chemical, petrochemical, construction, etc) is constantly increasing, thanks to its good mechanical properties combined with its excellent resistance to corrosion. However, a particular study is needed when DSSs applications involve intermediate temperatures. This is because DSSs are prone to thermal embrittlement in the range between 300°C and 500°C, the so-called "475 °C embrittlement." This phenomenon is ascribed to the spinodal decomposition (SD) of the ferritic phase into chromium-rich α′ and iron-rich α regions.[1,2] After prolonged ageing treatment at intermediate temperatures, together with SD, G-phase precipitation is generally observed[3-5] contributing to the steel embrittlement. However, it should be considered that the precipitation of G phase will be promoted more actively with the increase of the availability of G phase forming elements (mainly Ni and Mo).[4] In addition, G-phase precipitation can only be seen after a certain level of SD in steels with Mo.[6]

Presently, one way to reduce the cost of DSS is to decrease the content of the most expensive elements of the alloy: nickel and molybdenum. These elements are partially replaced by increases in manganese and nitrogen

Nomenclature: AG, The materials subject to a thermal ageing for 100 h at 475°C will be called "aged"; AL 2003, UNS S32003; AR, The steels supplied after the industrial process will be referred to as "as-received"; Cr_{eq}, Chromium equivalent; DSSs, Duplex Stainless Steels; EDS, Energy dispersive X-ray spectroscopy; LDSSs, Lean Duplex Stainless Steels; LCF, Low cycle fatigue; LDX 2101, UNS S32101; Ni_{eq}, Nickel equivalent; SAF 2507, UNS S32750; SD, Spinodal decomposition; SFE, Stacking-fault energy; STEM, Scanning transmission electron microscopy; TEM, Transmission electron microscope; YS, yield strength; α, Ferrite; α′–α, Chromium-rich and iron-rich regions; γ, Austenite; $\Delta\varepsilon_p$, Plastic strain range; $\dot{\varepsilon}$, Strain rate

content to maintain the proportions of phases. The development of more economic DSSs leads to the so-called Lean DSSs (LDSSs).[2,7] In addition to temperature, the chemical composition affects the kinetics of SD of the ferrite phase. In particular, elements such as Cr, Ni, Ti, Cb, Si, Al, Mo, C, N, and P have been reported to hasten the kinetics of the α–α′ phase separation.[8-11] Taking this into account, there is evidence that standard DSSs are more susceptible to suffer SD than LDSSs. Accordingly, Tucker et al[12] reported that the lower concentrations of Cr equivalent (Cr_{eq}) and Ni equivalent (Ni_{eq}) in LDSS delay the onset of α–α′ phase separation in comparison to standard DSS. Several expressions of Cr_{eq} and Ni_{eq} have been developed since 1946 when Campbell and Thomas first proposed the concept of Cr_{eq} during the microstructual study of welded alloy 25Cr-20Ni.[13,14] Today, the expressions derived from the WRC-92 diagram are the most widely used for duplex and austenitic stainless steels (Equations 1 and 2).

$$Cr_{eq} = \%Cr + \%Mo + 0.7\ x\%Nb \quad (1)$$

$$Ni_{eq} = \%Ni + 35\ x\%C + 20\ x\%N + 0.25\ x\%Cu \quad (2)$$

Since the crystal structure and lattice parameters of α and α′ phase are nearly the same (α: 2.866 Å; α′: 2.885 Å),[15] it is very be difficult to differentiate by optical metallography and X-ray diffractometry the domains rich in Cr and rich in Fe.[13,16] Because of the high coherency of α and α′, the fine scale microstructural decomposition of the ferrite (2-6 nm) is also difficult to characterize by transmission electron microscope (TEM). However, in most cases, mottled contrast, which has the appearance of an orange peel, can still be observed by TEM.[17] Over the last decades, many materials characterization instruments have been vastly improved, and simultaneously, a number of new techniques have emerged. Among these techniques are Atom Probe Field Ion Microscopy and Atom Probe Tomography, which have been widely used to obtain an atomic level microstructural characterization of SD.[1,9,18-20] On the other hand, scanning transmission electron microscopy (STEM) in combination with energy dispersive X-ray spectroscopy (EDS) provides both microstructure and microchemical mapping of materials at nanometer scale. Thus, chemical mapping of nanoparticles can be efficiently obtained with STEM-EDS. Therefore, STEM-EDS analysis is a very useful technique to study the SD.[21] In literature, thermal ageing effects on the fatigue behaviour of DSSs have been extensively investigated.[21-27] In recent years, although studies addressing the thermal embrittlement in LDSSs[8,11,12,28] are documented, no information related to the cyclic response and accompanying substructure of aged LDSS could be found from the published data. Thus, it is the purpose of this work to study the effect of thermal ageing on the fatigue behaviour of 2 LDSSs with different Cr_{eq} and Ni_{eq}. Moreover, the correlation between the fatigue behaviour and the dislocation structure in both phases is attempted.

2 | MATERIAL AND EXPERIMENTAL PROCEDURE

2.1 | Materials

The investigated materials were 2 LDSSs, LDX 2101 (UNS S32101) and AL 2003 (UNS S32003). These materials were chosen, taken into account their different Cr_{eq} and Ni_{eq}. The LDSS AL 2003 has a chemical composition more similar to standard DSSs while LDX 2101 is more representative of LDSSs. Table 1 gives the chemical composition in weight percent of both LDSSs and of SAF 2507 (UNS S32750). The chemical composition of this last DSS grade was added for comparison purposes.

The LDSSs were received in longitudinally welded stainless steel pipes. The manufacturing process of the pipes includes a hot rolled stage and a subsequent welding of the tube. A thermal treatment at 1050°C followed by a rapid water quench was finally performed to the tube. The steels supplied after this industrial process will be hereinafter referred to as "as-received" (AR). In this condition, a lamellar structure of bright austenite islands embedded in a grey etched ferrite matrix is distinguished in the rolling direction with no evidence of any additional secondary phases.[29,31] Table 2 shows the average grain size and volume fraction of each phase in both LDSSs and in DSS SAF 2507, for comparison purposes. These microstructural features were determined in previous studies.[29,30] Table 3 shows the Cr_{eq} and Ni_{eq} for the studied LDSSs and for SAF 2507; these amounts were determined using the equations specified above (Equations 1 and 2).

TABLE 1 Nominal composition of LDX 2101, AL 2003, and SAF 2507 in weight percent (wt%)

Material	C	Si	Mn	P	S	Ni	Cr	Mo	Cu	N
LDX 2101	0.026	0.63	4.9	0.021	0.001	1.53	21.53	0.28	0.33	0.22
AL 2003	0.021	0.22	1.73	0.024	—	3.8	22	1.8	—	0.18
SAF 2507	0.015	0.21	0.72	0.025	0.001	7.13	24.97	3.8	0.25	0.247

TABLE 2 Grain size and volume fraction of phases in AR-LDSSs[29] and in AR-SAF 2507[30]

Material	Phase	Average diameter (μm)	Volume Fraction of Phases
AR-LDX2101	Ferrite	4	0.31
	Austenite	5	0.69
AR-AL2003	Ferrite	7	0.48
	Austenite	4	0.52
SAF 2507	Ferrite	10	0.46
	Austenite	5	0.54

TABLE 3 Cr_{eq} and Ni_{eq} of LDX 2101, AL 2003, and SAF 2507

Material	Cr_{eq}	Ni_{eq}
LDX2101	21.8	6.9
AL2003	23.8	8.1
SAF 2507	28.7	12.8

2.2 | Specimen preparation

Slabs of LDSSs were cut from the pipes, in the direction parallel to its axis. Some slabs were thermal treated for 100 hours at 475°C. The material subject to this ageing treatment will henceforth be called "aged" (AG). From AR and AG materials, flat specimens for low cycle fatigue (LCF) were prepared by electro erosion with a 20-mm gauge length and a section of 30 mm^2. To obtain a smooth surface for the fatigue tests, all the specimens were initially ground and polished with sequentially finer grits (from 60 down to 1200 grid SiC paper).

2.3 | Mechanical tests

Low cycle fatigue tests were performed with an electromechanical testing machine Instron mod 1362 at room temperature under plastic strain control, applying a fully reversed triangular waveform at a constant total strain rate of $\dot{\varepsilon} = 2 \text{ x } 10\text{-}3 \text{ s}^{-1}$, with a plastic strain range of $\Delta\varepsilon_p = 0.2\%$.

2.4 | Microhardness

Vickers microhardness was measured in each phase of AR and AG samples of LDSSs. The indentations were performed with a load of 245.2 mN during 10 seconds. Care was taken that the indentations laid inside each phase. A minimum of 10 measures were performed. With these results thereafter, the corresponding medium value with its standard deviation was calculated.

2.5 | Microstructure observation

A FEI Tecnai F20-ST field emission gun microscope operated at 200 kV equipped with energy dispersive X-ray device, a systematic combination of images techniques (STEM) and chemical analysis (EDS) using a subnanometre probe (1-2 nm) was utilized to study the SD.

To analyse the dislocation structure, thin foils were prepared from discs cut parallel to the tensile axis of the specimen. The dislocation structures of the specimens cycled up to failure were observed in a conventional TEM (Philips EM300) operating at 100 kV.

3 | RESULTS AND DISCUSSION

Figures 1 and 2 show the characteristic dislocation microstructure of both LDSSs in AR and AG condition, respectively. The thermomechanical manufacturing process of the pipes has left a high dislocation density mainly in the ferrite phase.[32] Accordingly, dense dislocation tangles are observed in the ferritic phase for both conditions: AR and AG. At this magnification, TEM observations of ferrite phase in AG samples do not give evidence of the mottled contrast characteristic of the SD. On the other hand, it should be noticed a pronounce increase of dislocation density in the austenite phase of AL 2003 after the ageing thermal treatment, Figure 2C. At higher magnification, in Figure 3, the mottled contrast associated with the segregation of Cr and Fe atoms can be slightly distinguished, but there is no evidence of G phase, in the ferrite phase of both LDSSs. The low Ni and Mo content present in LDSS and the short time implemented for its ageing can explain the absence of G phase.

According to several previous works, the thermal ageing of DSSs and LDSSs at 475°C only affects the ferrite phase.[11,12,15,17,33] In this respect, it is well documented that the ferrite phase is noticeably hardened by ageing, whereas the hardness of the austenite is nearly unaffected.[11] Table 4 shows the Vickers microhardness values of ferrite and austenite phases of both LDSSs in the AR and AG conditions. The hardness of DSS 2507 is also

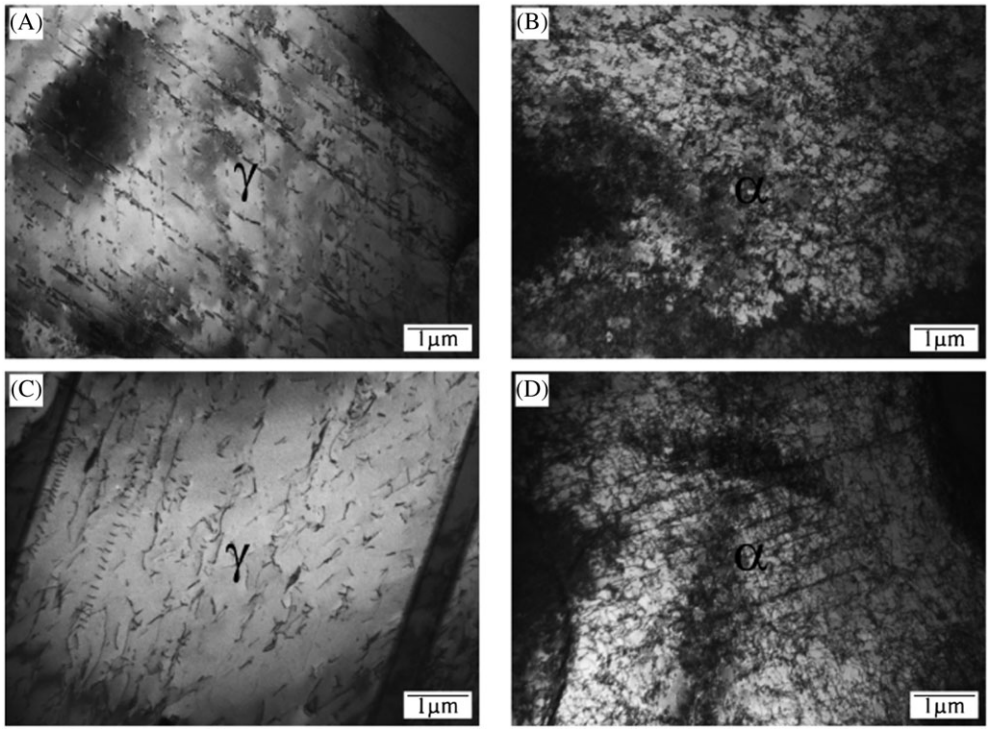

FIGURE 1 Dislocation microstructure of A, B, AR-LDX 2101 and C, D, AR-AL 2003

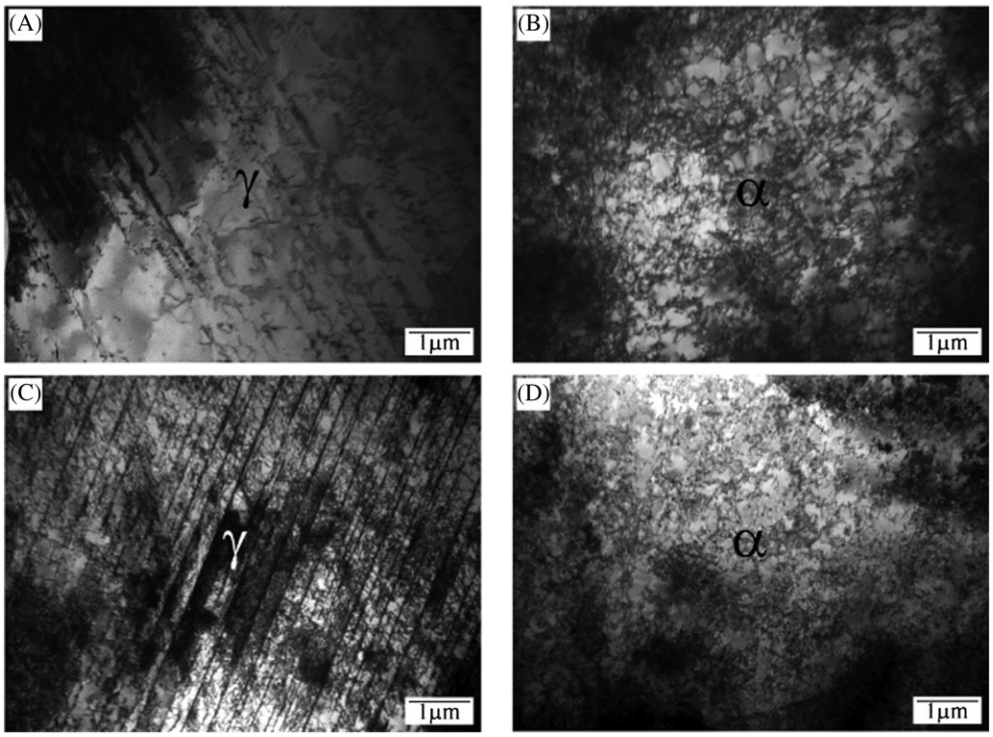

FIGURE 2 Dislocation microstructure of A, B, AG-LDX 2101 and C, D, AG-AL 2003

added to Table 4 for comparison purposes.[34] The hardness of LDX 2101's phases shows the usual trends, ie, the hardness of the ferrite increases with ageing while the hardness of the austenite remains unchanged. Surprisingly, in the AL 2003, both phases suffer a pronounced hardness increase with the ageing treatment. Merlo et al[35] have already found this result in aged LDSS UNS S32304. However, they do not point out this phenomenon as curious nor they explain its occurrence. In the present work, the hardness increase in the austenite phase of AL 2003 could

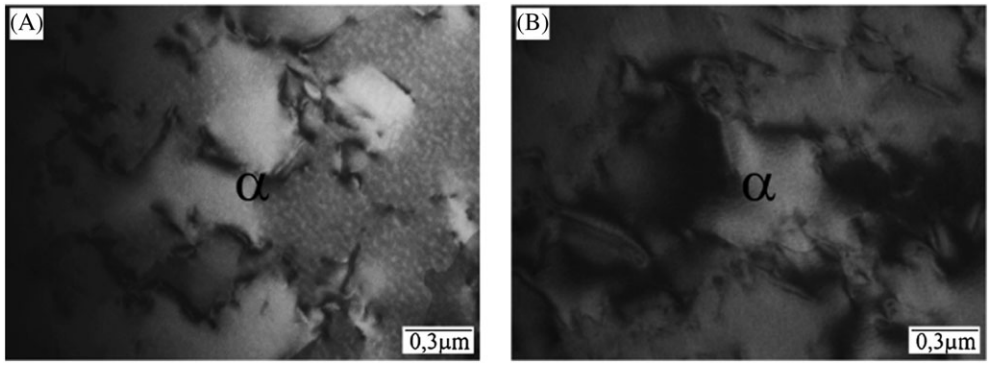

FIGURE 3 Mottled contrast associated with the SD in A, AG-LDX 2101 and B, AG-AL 2003

be associated to an increase in the dislocation density, Figure 1C and Figure 2C. Taking into account that the difference in thermal expansion coefficient between α and γ phases is larger at intermediate temperatures than at room temperature,[36] when DSSs are cooled down from 475°C to room temperature, internal stresses could be generated. Figure 2C suggests that the austenite phase accommodate this misfit strain. The distribution of strain between austenite and ferrite in DSS under an applied stress is highly complex.[37,38] On the other hand, strain partitioning in duplex microstructures subjected to thermal treatments can be explained qualitatively by the mechanical behaviour of 2-phase materials.[39,40] These studies indicate that in microstructures containing hard inclusions, the matrix supports most of the plastic deformation, whereas in microstructures with weak inclusions, both phases are plastically deformed. In this sense, DSS could be considered as a composite steel where the austenite can be considered as the matrix and the aged ferrite grains as the inclusions. Thus, in aged DSSs, the hardened ferrite could induce the austenite to bear the misfit strain originated by the internal stresses due to the difference in thermal expansion of the phases. In support of this assumption, several aspects should be considered. First, the yield stress of the austenite phase in each DSS will limit the plastic strain found in this phase. It has been reported[41] that the 0.2% yield strength (YS) of austenitic and DSSs follows the equation:

$$YS(MPa) = 120 + 210\sqrt{N + 0.02} + 2Mn + 2Cr + 14Mo + 10Cu + (6.15\text{-}0.054\delta)\delta + (7 + 35(N + 0.2))d^{-1/2}, \quad (3)$$

Where, d is grain diameter in millimeters, and δ is percent ferrite. The stated accuracy for this equation is 20 MPa. Taking in consideration the chemical compositions obtained by EDS analysis (Table 5) and the estimation of the nitrogen content (detailed in Table 5), the YS of austenitic phase of LDX 2101, AL 2003, and SAF 2507 was evaluated using Equation 3, the YS values are 650, 700, and 810 MPa, respectively. In view of these results, it could be inferred that the internal stresses would be enough to the produce the plastic deformation of the γ grains in the LDSSs but not in the standard DSS. The above assumption is in line with the usually reported unchanged harness and dislocation density in the austenite phase of aged standard DSSs. Although both studied LDSSs have similar YS for austenite, only AG-AL2003

TABLE 4 Vickers microhardness of both LDSSs and DSS SAF 2507[25] in AR and AG conditions

Material (HV)	Ferrite (HV)	Austenite (HV)
AR-LDX2101	260 ± 10	330 ± 20
AG-LDX2101	340 ± 10	340 ± 10
AR-AL2003	310 ± 10	320 ± 20
AG-AL2003	370 ± 10	390 ± 10
AR-SAF 2507	350 ± 20	360 ± 20
AG-SAF 2507	470 ± 20	350 ± 20

Abbreviations: AG, aged; AR, as-received; DSSs, duplex stainless steels; LDSSs, lean DSSs.

TABLE 5 Chemical analysis of the main elements in ferrite and austenite of LDX 2101, AL 2003, and SAF 2507 in weight percent (wt%)

Material	Phase	Cr[a]	Mn[a]	Ni[a]	Cu[a]	Mo[a]	N[b]
LDX 2101	Austenite	21.57	5.07	2.64	0.52	0.54	0.298
	Ferrite	23.30	4.55	1.97	0.25	0.57	
Al 2003	Austenite	21.41	1.96	5.36	0.30	1.51	0.305
	Ferrite	23.80	1.75	3.61	0.28	2.18	
SAF 2507	Austenite	0.015	0.21	0.72	0.025	0.001	0.484
	Ferrite	27.12	0.36	5.72	0.30	5.85	

[a]Energy dispersive X-ray spectroscopy (EDS).

[b]Calculated, assuming that the solubility limits of Nitrogen in the ferrite phase is 0.045% wt[42], by the following equation: N in austenite in weight percent (wt%) = (N in the nominal composition in wt% - Solubility limit of N in the ferrite × Volume fraction of ferrite) / Volume fraction of austenite.

shows evidences of plastic deformation, Figure 1C, Figure 2C, and Table 4. However, it seems that this is not the case for AG-LDX 2101 as neither the dislocation density nor the hardness of austenite phase changes after the ageing treatment (Figures 1A, 2A, and Table 4). This fact can be explained considering that the stresses arising from the difference of thermal expansion coefficient between phases are accommodated by a larger volume fraction of austenite in the AG-LDX 2101 than in AG-AL 2003 (Table 2).

Figure 4 shows the EDX compositional profile obtained using a nanometric probe of both AG-LDSSs. For comparison purposes, the EDX compositional profile of DSS SAF 2507[21] aged at 475°C for 100 hours was added to Figure 4. From this figure, it becomes evident that the compositional amplitude fluctuations caused by SD are really higher in the DSS than in LDSSs. This result agrees with the influence of Cr_{eq} and Ni_{eq} (Table 3) on SD already reported in other DSSs. Furthermore, the higher Cr_{eq} and N_{ieq} values of AL 2003 (Table 3) suggest that its ferrite phase should hasten the SD in comparison with LDX 2101. However, no significant difference between the SD in both AG-LDSSs is found in Figure 4.

Figure 5 shows the cyclic hardening-softening responses of LDSSs in AR and AG conditions at $\Delta\varepsilon_p = 0.2\%$. It should be noted that the general cyclic behaviour of both LDSSs is characterized by a cyclic softening during the whole fatigue life. However, the LDSS AL 2003 attains higher stress levels than LDX 2101 in both conditions. As it was already established in a previous work,[32] the higher stress attained by AR-AL 2003 than by AR-LDX 2101 could be attributed to the higher hardness of the ferrite phase in AR-AL 2003, due to its higher molybdenum content. Something worthy of note is that the ageing treatment causes a larger increase in

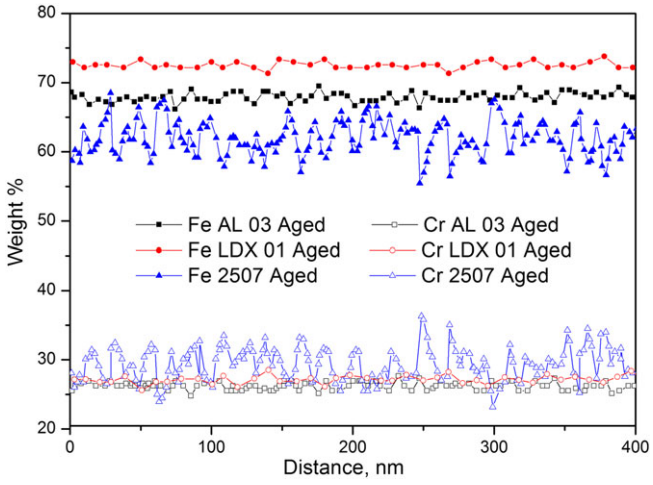

FIGURE 4 Compositional profile of ferrite phase in aged LDSSs and DSS SAF 2507 [Colour figure can be viewed at wileyonlinelibrary.com]

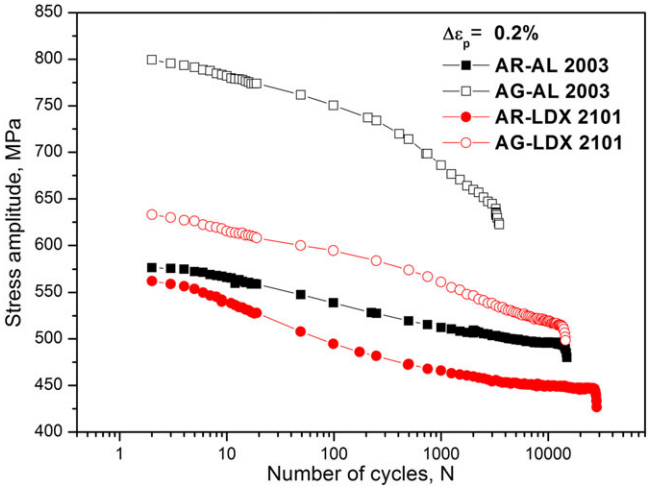

FIGURE 5 Cyclic behaviour of AR and AG-LDSSs at $\Delta\varepsilon_p = 0.2\%$ [Colour figure can be viewed at wileyonlinelibrary.com]

the stress amplitude in AL 2003 than in LDX 2101 relative to the AR conditions. Because of ageing, both phases hardened in AL 2003 while only the ferrite phase hardened in LDX 2101 (Table 4). This fact can explain the different mechanical behaviour observed between both AG-LDSSs. It is really important to remark that the ageing treatment not only is beneficial in improving the strength of the present LDSSs but also does not deteriorate the fatigue life considerably. A higher detrimental effect on the fatigue life is observed in AG-AL 2003 that in AG-LDX2101. Thus, with an adequate volume fraction of phases in LDSSs, the ageing treatment leads to an increase in strength without causing a great detriment in fatigue life.

To correlate the mechanical behaviour with the dislocation structure of fatigued specimens, thin foils were prepared from specimens cycled up to failure. It is well-known that nitrogen in solid solution in the austenite phase promotes the development of planar arrays of dislocations, which enhances cyclic softening.[43] Consequently, the microstructure observed in the austenite of fatigued AR-LDSSs is characterized by planar slip Figure 6A and 6C. It is also important to consider that the elastoplastic properties and the distribution of the load between the phases in DSSs affect the amount of plastic strain supported by each phase during the fatigue test.[44] In this sense, Strubbia et al[29] found that in AR-LDX 2101 during LCF, the ferrite experiences a higher plastic deformation than the austenite as the austenite is initially harder than ferrite. This result is in agreement with those found in this work, (Figure 6A and 6B). In the austenite phase of AR-AL2003, there is a reduce mobility of screw dislocations by nitrogen.

Accordingly, it is easier for the ferrite phase of AR-AL2003 to accommodate most of the deformation (Figures 6C and 6D). In summary, the present work

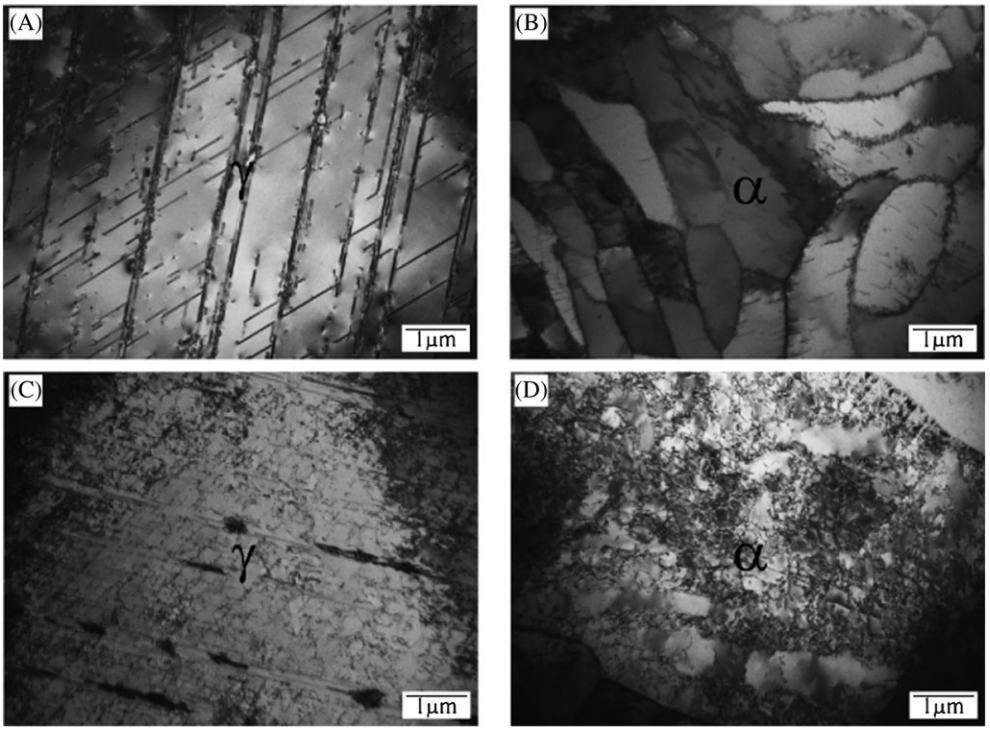

FIGURE 6 Dislocation microstructure of A, B, fatigued AR-LDX 2101 and C, D, fatigued AR-AL 2003

provides further proof of the preponderant role of the ferrite phase in strain partitioning of AR-LDSSs during LCF. This fact is based on the microstructural evolution from a statistically distributed dislocation structure (Figure 1B and 1D) to a cell structure (Figure 6B and 6D) in the ferrite phase and the nearly negligible microstructural changes in the austenite phase during the fatigue tests (Figures 1A, 1C, 6A, and 6 C). Conversely, in AG-LDSSs, the austenite phase seems to bear most of the plastic deformation during LCF (Figure 7). This deformation

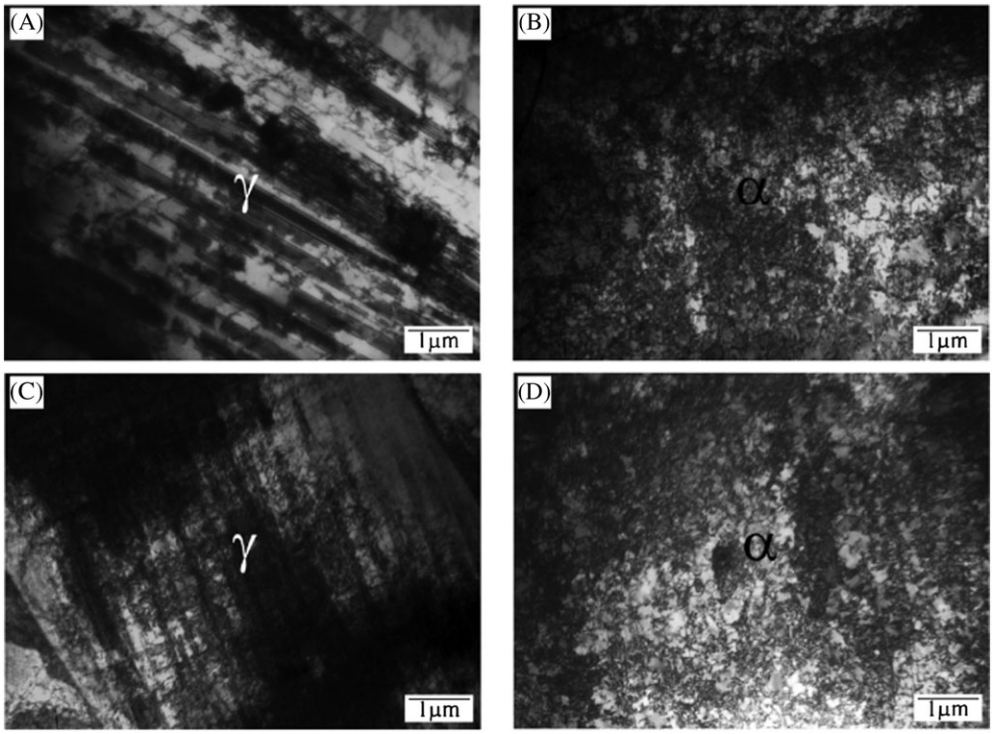

FIGURE 7 Dislocation microstructure of A, B, fatigued AG-LDX 2101 and C, D, fatigued AG-AL 2003

strain partition is mainly a consequence of restricted dislocation motion in the decomposed ferrite phase. Marinelli et al[45] also found that the high yield stress required to plastically deform the embrittled ferrite of aged DSS SAF 2205 makes the austenite the only phase capable to accommodate the deformation.

As regards AG-LDSSs fatigued, the ferritic dislocation substructure has not changed significantly, although a few ferritic grains of AG-LDX 2101 develop dislocations bands and microbands (Figure 8). A similar type of dislocation arrangement was found by Hereñú et al[21] in the ferrite phase of aged DSS SAF 2507 cycled at room temperature. Conversely, the austenite phase of AG-LDSSs has developed a more evolved structure during fatigue. Although the austenite of both AG-LDSSs displays a planar slip character, some differences should be pointed out. Whereas in AG-LDX 2101, the cyclic plasticity is mainly accommodated by stacking faults; in AG-AL2003, the microstructure is characterized by stacking faults and dislocations packed into bands. The steels deformation mode is linked to the stacking-fault energy (SFE), which is compositional dependent. It should be considered that the width of the stacking fault "ribbon" is inversely proportional to the value of the SFE.[46] Therefore, the comparison of the austenite microstructure of LDSSs (Figure 6A and 6C) suggests that the SFE is higher in the AL 2003. Moreover, a small amount of ε-martensite was observed in the austenitic grains of AG-LDX2101 cycled (Figure 9), not causing observable effect on the fatigue behaviour. Finally, it can be concluded that the LDSS with lower Cr_{eq} and Ni_{eq} values exhibits improved fatigue properties in both conditions AR and AG.

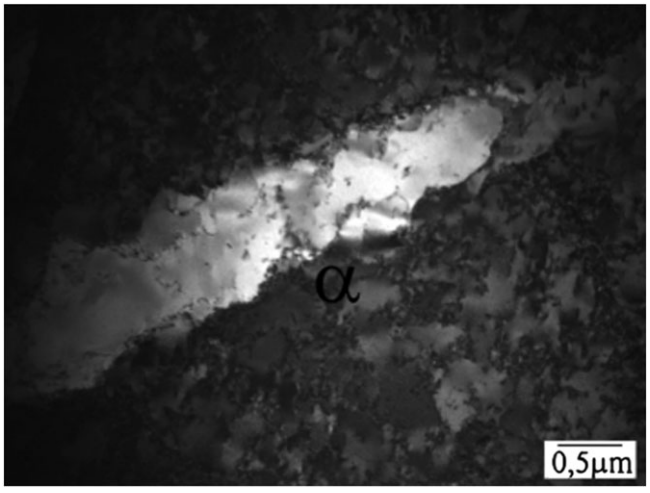

FIGURE 8 Dislocations microbands in a ferritic grain of AG-LDX 2101 cycled

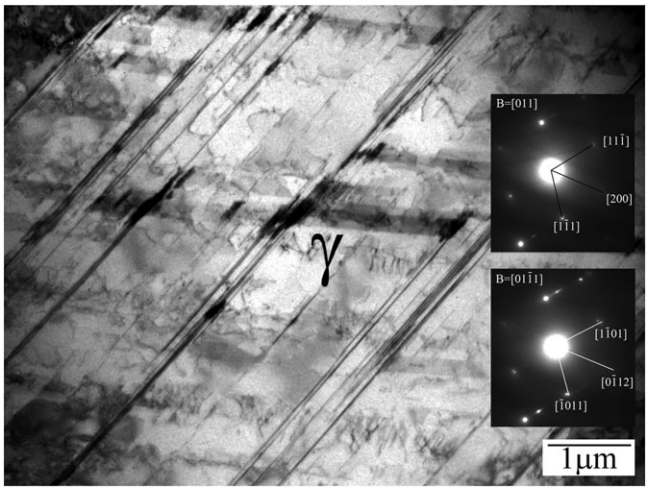

FIGURE 9 ε-Martensite present in an austenitic grain of AG-LDX2101 cycled

4 | CONCLUSIONS

The following conclusions about thermal ageing's effect on the fatigue behaviour of 2 LDSSs can be drawn:

The compositional amplitude fluctuations caused by SD are higher in the standard DSS than in Lean DSSs. Moreover, this amplitude is similar in both Lean DSSs.

In AL 2003, the thermal ageing leads to a pronounced hardening of both phases and an increase of dislocation density in the austenite phase. On the other hand, in LDX 2101, the thermal ageing only increases the hardness of the ferrite phase. The dissimilar between these LDSSs can be explained by the misfit strain originated by the internal stresses due to the difference in thermal expansion of the phases and by the volume fraction of austenite in each LDSSs.

During LCF, the ferrite phase has a preponderant role in strain partitioning of AR-LDSSs, while in AG-LDSSs, the austenite phase bears most of the plastic deformation. A small amount of ε-martensite induced by cycling in AG-LDX2101 does not affect the fatigue behaviour.

The thermal ageing treatment causes improved fatigue properties in LDX2101.

ACKNOWLEDGEMENT

This work was supported by Consejo Nacional de Investigaciones Científicas y Técnicas (2014-2017 PICT-2013-1105) of Argentina.

ORCID

Renata Strubbia http://orcid.org/0000-0002-9444-7799
Mohamed Sennour http://orcid.org/0000-0002-2885-5866
Silvina Hereñú http://orcid.org/0000-0003-0648-5654

REFERENCES

1. Danoix F, Auger P. Atom probe studies of the Fe–Cr system and stainless steels aged at intermediate temperature: a review. *Mater Charact*. 2000;44:177-201.
2. Alvarez-Armas I, Degallaix-Moreuil S (Eds). *Duplex Stainless Steels*. ISTE Ltd., London, Uk and John Wiley & Sons Inc., Hoboken, USA; 2009.
3. Danoix F, Auger P, Chambreland S, Blavette D. A 3D study of G-phase precipitation in spinodally decomposed α-ferrite by tomographic atom-probe analysis. *Microsc Microanal Microstruct*. 1994;5(April):121-132.
4. Di Cocco V, Iacoviello F, Ischia G. Duplex stainless steels "475°C embrittlement": influence of the chemical composition on the fatigue crack propagation. *Procedia Struct Integr*. 2017;3:299-307.
5. Maetz J-Y, Cazottes S, Verdu C, Danoix F, Kléber X. Microstructural evolution in 2101 lean duplex stainless steel during low- and intermediate-temperature aging. *Microsc Microanal*. 2016;22(2):463-473.
6. Gironès Molera, A. (2003) Influence of environment and temperature on the low cycle fatigue properties of superduplex stainless steels.
7. Kumar A. (2008) Development and characterization of nickel free duplex stainless steel, Thapar University. http://dspace.thapar.edu:8080/dspace/bitstream/10266/555/3/T555.pdf.
8. Tucker JD, Miller MK, Young GA. Assessment of thermal embrittlement in duplex stainless steels 2003 and 2205 for nuclear power applications. *Acta Mater*. 2015;87:15-24.
9. Hedström P, Huyan F, Zhou J, Wessman S, Thuvander M, Odqvist J. The 475°C embrittlement in Fe–20Cr and Fe–20Cr–X (X=Ni, Cu, Mn) alloys studied by mechanical testing and atom probe tomography. *Mater Sci Eng A*. 2013;574:123-129.
10. Wasserman FG, Tavares SSM, Pardal JM, Mainier FB, Faria RA, Nunes CS. Effects of low temperature aging on the mechanical properties and corrosion resistance of duplex and lean duplex stainless steels UNS S32205 and UNS S32304. *Rem Rev Esc*. 2013;66(2):193-200.
11. Silva R, Baroni LFS, Silva MBR, Afonso CRM, Kuri SE, Rovere CA. Effect of thermal aging at 475 C on the properties of lean duplex stainless steel 2101. *Mater Charact*. 2016;114:211-217. https://doi.org/10.1016/j.matchar.2016.03.002
12. Tucker JD, Young GA Jr, Eno DR. Thermal embrittlement of a lean grade of duplex stainless steel: alloy 2003. *Solid State Phenom*. 2011;172–174:331-337.
13. Lai J, Shek C, Lo K. *Stainless Steels: An Introduction and Their Recent Developments*. Bentham Science Publishers; 2012.
14. Bermejo MAV. Predictive and measurement methods for delta ferrite determination. *Weld J*. 1999;91(April):113-121.
15. Weng K, Chen H, Yang J. The low-temperature aging embrittlement in a 2205 duplex stainless steel. *Mater Sci Eng A*. 2004;379(1–2):119-132.
16. Lo KH, Lai JKL. Microstructural characterisation and change in a.C. Magnetic susceptibility of duplex stainless steel during spinodal decomposition. *J. Nucl. Mater.* 2010;401:143-148. https://doi.org/10.1016/j.jnucmat.2010.04.014
17. Huyan F. *A study of "475 embrittlement" in Fe-20Cr and Fe-20Cr-X (X=Ni, Cu, Mn) alloys*. Sweden: Stockholm; 2012 http://www.diva-portal.se/smash/get/diva2:604942/FULLTEXT01.pdf.
18. Pareige C, Emo J, Saillet S, Domain C, Pareige P. Kinetics of G-phase precipitation and spinodal decomposition in very long aged ferrite of a Mo-free duplex stainless steel. *J Nucl Mater*. 2015;465:383-389.
19. Nilsson J, Chai G. The physical metallurgy of duplex stainless steels. 8th Duplex Stainl. Steels Conf. 2010.
20. Krupp U, Söker M, Giertler A, et al. The potential of spinodal ferrite decomposition for increasing the very high cycle fatigue strength of duplex stainless steel. *Int J Fatigue*. 2016;93:363-371.
21. Hereñú S, Sennour M, Balbi M, Alvarez-Armas I, Thorel A, Armas AF. Influence of dislocation glide on the spinodal decomposition of fatigued duplex stainless steels. *Mater Sci Eng A*. 2011;528(25–26):7636-7640.
22. Llanes L, Mateo A, Iturgoyen L, Anglada M. Aging effects on the cyclic deformation mechanisms of a duplex stainless. *Acta Mater*. 1996;44(10):3967-3978.
23. Sahu JK, Ghosh RN, Christ H-J. Low cycle fatigue behaviour of duplex stainless steel: influence of isothermal aging treatment. *Fatigue Fract Eng Mater Struct*. 2010;33(2):77-86.
24. 1. Stolarz J, Foct J. Specific features of two phase alloys response to cyclic deformation. *Mater Sci Eng A*. 2001;319–321:501-505.
25. Balbi M, Avalos M, El Bartali A, Alvarez-Armas I. Microcrack growth and fatigue behavior of a duplex stainless steel. *Int. J. Fatigue*. 2009;31(11–12):2006-2013. https://doi.org/10.1016/j.ijfatigue.2008.12.007
26. Chen W, Xue F, Tian Y, Yu D, Yu W, Chen X. Effect of thermal aging on the low cycle fatigue behavior of Z3CN20.09M cast duplex stainless steel. *Mater Sci Eng A*. 2015;646:263-271.
27. Armas AF, Hereñú S, Alvarez-Armas I, Degallaix S, Condó A, Lovey F. The influence of temperature on the cyclic behavior of aged and unaged super duplex stainless steels. *Mater Sci Eng A*. 2008;491(1–2):434-439.
28. Garfinkel DA, Poplawsky JD, Guo W, Young GA, Tucker JD. Phase separation in lean-grade duplex stainless steel 2101. 2015. Jom, 67;2216–22.
29. Strubbia R, Hereñú S, Alvarez-Armas I, Krupp U. Short fatigue cracks nucleation and growth in lean duplex stainless steel LDX 2101. *Mater Sci Eng A*. 2014;615:169-174.
30. Marinelli MC, Moscato MG, Signorelli JW, Bartali AE, Alvarez-Armas I. K-S relationship identification technique by EBSD. *Key Eng Mater*. 2011;465:415-418.
31. Strubbia R, Hereñú S, Giertler A-AI, Krupp U. Experimental characterization of short crack nucleation and growth during cycling in lean duplex stainless steels. *Int J Fatigue*. 2014;65:58-63.
32. Strubbia R, Hereñú S, Marinelli MC, Alvarez-Armas I. Short crack nucleation and growth in lean duplex stainless steels fatigued at room temperature. *Int J Fatigue*. 2012;2003:1-5.
33. Sahu JK, Krupp U, Ghosh RN, Christ H-J. Effect of 475°C embrittlement on the mechanical properties of duplex stainless steel. *Mater Sci Eng A*. 2009;508:1-14.

34. Hereñú S, Alvarez-Armas I, Armas A, Degallaix S, Condó A, Lovey F. Microstructural changes in a duplex stainless steel during low cycle fatigue*. *Mater Test*. 2009;51:359-364.

35. Merlo PP, Milagre MX, Machado CSC, Macêdo MCS, Orlando MT. Correlação entre a Resistência à Corrosão e as Tensões Residuais de um Aço Inoxidável Lean Duplex UNS S32304 Tratado Termicamente. An. do VI Encontro Científico Física Apl., 2015;116–120

36. Kaye and Layby Online (16th Ed.), National Physics Laboratory, Chapter 2.3.5 Thermal 28Moverare JJ, Ode M. Deformation behaviour of a prestrained duplex stainless steel. *Mater Sci Eng A*. 2002;337:25-38.

37. Moverare JJ, Ode M. Deformation behaviour of a prestrained duplex stainless steel. *Mater Sci Eng A*. 2002;337:25-38.

38. Johansson J, Oden M, Zeng X-H. Evolution of the residual stress state in a duplex stainless steel during loading. *Acta Mater*. 1999;47(9):2669-2684.

39. Bao G, Hutchinson JW, McMeeking RM. The flow stress of dual-phase, non-hardening solids. *Mech Mater*. 1991;12:85-94.

40. Fischmeister HF, Karlsson B. Plastizitatseigenschaften grob-zweiphasiger Werk-stoffe. *Z Metallkd*. 1997;68:311-327.

41. Nordberg H. Mechanical properties of austenitic and duplex stainless steels, In 1st European Stainless Steel Conference. Processes and Materials Innovation Stainless Steel, 1993;2:217–230.

42. Moreno I, Almagro JF, Llovet X. Determination of nitrogen in duplex stainless steels by EPMA. *Mikrochim Acta*. 2002;139:105-110.

43. Vogt J-B. Fatigue properties of high nitrogen steels. *J Mater Process Technol*. 2001;117:364-369.

44. Lillbacka R, Chai G, Ekh M, Liu P, Johnson E, Runesson K. Cyclic stress–strain behavior and load sharing in duplex stainless steels: aspects of modeling and experiments. *Acta Mater*. 2007;55(16):5359-5368.

45. Marinelli MC, Krupp U, Kübbeler M, Hereñú S, Alvarez-Armas I. The effect of the embrittlement on the fatigue limit and crack propagation in a duplex stainless steel during high cycle fatigue. *Eng Fract Mech*. 2013;110:421-429.

46. Smallman RE, Bishop RJ. *Modern Physical Metallurgy and Materials Engineering Science, Process, Applications*. Oxford: Butterworth-Heinemann; 1999.

How to cite this article: Strubbia R, Sennour M, Hereñú S. Effect of 475°C embrittlement on the low cycle fatigue behaviour of lean duplex stainless steels. *Fatigue Fract Eng Mater Struct*. 2018;41:473–482. https://doi.org/10.1111/ffe.12714